International Journal on Science and Technology (IJSAT)

E-ISSN: 2229-7677 ● Website: www.ijsat.org ● Email: editor@ijsat.org

Advances in Synthetic Aperture Radar Image Change Detection: Challenges and Innovations

Himani Prajapati[1], Dr.Vibha Patel[2]

[1]Master's in Information Technology, Vishwakarma Government Engineering College, Gujarat, India
[2]HOD in Information Technology, Vishwakarma Government Engineering College, Gujarat, India

Abstract

One of the most crucial areas of study in remote sensing is the detection of changes in Synthetic Aperture Radar images, which finds use in disaster relief and environmental monitoring. The study presents an analysis of machine learning techniques in SAR image change detection. Traditional methods, which consist of image differencing followed by thresholding, are introduced. Novel supervised change detection models based on feature representation learning using convolutional neural networks are proposed. A detailed presentation of a few unsupervised models follows. An innovative network design for detecting changes in Synthetic Aperture Radar images is the Siamese Adaptive Fusion Network (SAFNet). This makes the problem challenging in SAR image change detection, mainly due to the complex multiscale feature fusion and limited correlation between multitemporal features. By using a two-branch CNN architecture to extract high-level semantic features from multitemporal SAR pictures and adaptively fuse them using a fusion module that takes use of complementary information at various feature levels, SAFNet overcomes these problems.

Keywords: Synthetic Aperture Radar, Change Detection, Siamese Adaptive Fusion Network (SAFNet), Deep Learning

1. Introduction

An essential challenge in remote sensing is the detection of changes in Synthetic Aperture Radar (SAR) pictures, which enables the identification of changes that have taken place between two or more multitemporal photographs of the same region [1]. SAR imaging systems are well renowned for their exceptional ability to capture high-resolution images in all weather, which makes them particularly useful in situations when optical sensors are impeded by haze, cloud cover, or poor illumination [2]. SAR change detection applications span from disaster response and environmental monitoring to urban planning and crop assessment. SAR change detection is a challenging problem despite its enormous potential, mostly because of the intrinsic speckle noise in SAR pictures, which adds unpredictability and lowers image quality [3]. Together with the difficulty of correlating features across different scales and temporal domains, this often hampers the effectiveness of traditional methods. These issues suggest the requirement of advanced approaches able to manage noise, extract meaningful features, and provide robust change detection results [4].

Three primary processes typically comprise the traditional change detection approaches for SAR: preprocessing, difference image (DI) production, and classification [5]. Preprocessing involves coregistration of the images to accurately align the temporal images. The creation of DIs using operators that highlight altered regions, such as the log-ratio, Gauss-ratio, or neighborhood-based ratio approaches, is the second stage. The last stage is classifying the DI into modified and unaltered classes using methods like fuzzy logic, thresholding, and clustering [6]. These approaches are simple and computationally efficient but very sensitive to noise and not capable of capturing complex patterns in high-dimensional data. Thus, they often yield unreliable change maps in challenging scenarios with heavy noise or subtle changes.

The Siamese Adaptive Fusion Network (SAFNet) is a novel deep learning framework that overcomes these limitations by proposing a new architecture specifically designed for SAR image change detection. SAFNet is constructed based on a dual-branch CNN structure, where each branch extracts high-level semantic features independently for one of the two input SAR images [7]. These features are further fused through an adaptive fusion module, the core innovation of SAFNet. The multiscale features extracted from different levels of the network are integrated into the fusion module with an attention mechanism, which dynamically weighs the importance of the features at different scales. This guarantees that the relevant features are emphasized while the irrelevant or redundant information is suppressed, thus leading to a more robust and accurate representation of the changes.

One of the most distinctive components of SAFNet is its correlation layer, which further enhances feature integration between the two branches. Traditional feature combination methods, such as summation or concatenation, usually cannot sufficiently exploit the relationships between multitemporal features, resulting in suboptimal performance. SAFNet's correlation layer, however, uses convolutional operations to capture intricate relationships between the features, allowing the network to better distinguish subtle changes from noise. This layer improves the network's capacity to classify areas that have changed and those that have not, in addition to improving the representation of generic features. The training of SAFNet is simultaneously regularized by a combination of similarity measures and classification losses, which ensures that the model learns both to discriminate the features effectively and to make accurate predictions. The effectiveness of SAFNet has been validated on several real-world SAR datasets, including the Ottawa, and the S1GFloods datasets, which contain various resolutions, and types of changes. Experimental results show that SAFNet outperforms traditional methods and contemporary deep learning models by a margin. The adaptive fusion module and correlation layer contribute most to its success, enabling the network to maintain stable and discriminative feature representations even in challenging conditions, such as high-noise or subtle-change regions. Other metrics, such as Percentage of Correct Classification (PCC), Mean Intersection over Union (mIOU), and Kappa Coefficient (KC), also prove the superiority of SAFNet, with higher accuracy [8].

Besides the quantitative advantages, SAFNet performs better in visualizing change detection results with clearer details. This preservation of fine details by the model makes it even more valuable when applied to those applications that need high accuracy in detecting changes and monitoring urban growth, impacts of natural disasters, and environmental changes, among others [9]. With its adaptive fusion of features across scales and robust correlation-driven approach, SAFNet largely mitigates false positives and false negatives and then derives highly reliable change maps that are useful for critical scenarios.

2. Related Study

Remote sensing change detection has been researched at length, and numerous deep learning models have been introduced to enhance accuracy and resilience. LANTNet is based on pseudo-labels, which are noisy and can adversely impact the optimization of the model. Although it specializes in the relationship between convolutional features, it tends to disregard finer spatial details, which weakens detection performance. Likewise, Gao et al. (2021) introduced the Deep Cascade Network (DCNet), which is overfitting and redundant feature-affected, affecting classification efficiency and model generalization. The deeper network in DCNet is more likely to cause exploding gradients, rendering training unstable, especially with large datasets.

Speckle noise is one of the most significant challenges in SAR image analysis, and it impacts models like the Local Descriptor Learning CNN proposed by Dong et al. (2019). Even when using local descriptors, the model is not extremely effective at denoising. Its use of pseudo-labels can be a source of error, resulting in increased misclassification rates. Li et al. (2024) proposed a change detection algorithm using Principal Component Analysis and Two-Level Clustering, but their method loses important feature information in dimension reduction and is very sensitive to noise with more false positives and misclassifications.

Another significant limitation of SAR change detection models is the incorporation of noisy marginal features, such as in the Dual-Domain Network (DDNet), whose detection performance is adversely affected. Seydi et al. (2022) introduced the Multi-Dimensional Deep Siamese Network, which needs a great many training samples, and lower data efficiency in limited data scenarios. Also, sample generation for this model may involve noise affecting the detection performance and yielding high misclassification rates. Wang et al. (2022) proposed the Graph-Based Knowledge Supplement Network (GKSNet), which heavily depends on external labeled data for knowledge transfer, which restricts its performance in low-label scenarios. In the same way, Wang et al. (2023) introduced the Improved Siamese U-Net, which has a tendency to ignore minor target changes and create blurry boundaries, diminishing its ability to identify subtle changes. In addition, its feature fusion process can cause semantic misalignment, making it harder to differentiate fine-grained differences in remote sensing images.

Another key problem with change detection models is the lack of labels, especially in the case of the Semi-Supervised Urban Change Detection model by Hafner et al. (2023), which is based on Sentinel-1 SAR and Sentinel-2 MSI data. The model is responsible for generalizing across multiple environments because of the lack of good multi-modal datasets. Amitrano et al. (2024) discussed the High-Resolution Representation-Based Siamese Network (SiHDNet), where it fails to catch small-area variations, and therefore, useful information is lost in small variations.

Dong et al. (2021) put forward the Multiscale Self-Attention Deep Clustering for the SAR Change Detection model, pointing out that speckle noise sensitivity is still a major limitation of change detection approaches. Since the model is unable to effectively eliminate speckle noise, it has a high rate of false positives. Finally, the issue of uniform detection accuracy in changed and unchanged data affects the Unsupervised SAR Change Detection Method Based on Stochastic Subspace Ensemble Learning proposed by Cui et al. (2019) with resulting unstable results.

3. Methodology

3.1 Change Detection Framework

Change detection in SAR pictures is detecting and pinpointing variations between two coregistered images acquired at separate periods. Consider two SAR images I1 and I2 taken at different time instances over the same geographic area. Our framework aims to produce an accurate binary change map M, where changed regions are shown while unaltered areas are suppressed. Our solution is based on the SAFNet architecture, as it enhances spatial feature representation along with deep feature fusion to make detection more robust. The framework is primarily divided into two parts as follows:

3.1.1 Feature Extraction and Representation Learning

A two-branch CNN for the extraction of multi-level semantic features is applied to the input SAR image pairs. Each branch processes one of the two images while learning a hierarchical representation at different scales. The network captures the low-level textures and high-level contextual information to distinguish between changed and unchanged regions effectively. The feature maps extracted can be expressed as in (1):

$$F_1^i = S_1\left(x_{t1}^i\right), \ F_2^i = S_2(x_{t2}^i) \quad (1)$$

Where S_1 and S_2 are CNN feature extractors to handle the input SAR image patches from each time step. Extracted feature maps, F_1^i and F_2^i, denote the representations of the input images x_{t1}^i and x_{t2}^i, respectively. These feature maps store important spatial and contextual information and allow the network to distinguish successfully between altered and unaltered areas in the SAR images.

To improve the learnt features' ability to discriminate, a similarity metric is included during the training phase. The similarity measure makes the model learn feature embeddings closer for regions that are unchanged and farther for regions that are changed, making the network better capable of perceiving subtle changes. Besides, attention mechanisms are used to emphasize informative regions and suppress redundant noise, which is a common issue in SAR images due to speckle noise and multipath scattering effects.

3.1.2 Feature Fusion and Classification

Following feature extraction from both input images, a correlation layer is formed to fuse and contrast them. The layer applies element-wise subtraction and concatenation of feature maps to emphasize difference between the two time steps. The fusion operation helps learn detailed feature representations, enabling the network to learn important transformations occurring in the scene.

The merging step is performed according to a correlation function, which is given in (2):

$$F_{\{merge\}}^i = C\left(F_1^i, F_2^i\right) = F_1^i \times F_2^i \quad (2)$$

Where C (·) is a correlation function utilized to combine the extracted features of the two image patches. The fusion operation is performed by applying a group convolution operation, with F_1^i as the input and F_2^i as the convolution kernel. This operation improves feature representation by removing the spatial interactions among the two feature maps so that the model is able to pay attention to significant changes and filter out unnecessary noise.

After feature fusion, a classification module containing fully connected layers and ReLU activation generates the final change map is shown in (3). It distinguishes changed pixels from the rest by using fully connected module as the supervised classifier and makes its training rely on the optimization by ground truth of the change map. Thus, residual connections, multi-scale feature fusion are taken into Improved SAFNet that is beneficial for improving the precision and recall values in the task of change detection.

$$F_{\{class\}}^i = \mathrm{ReLU}\left(W_c F_{\{merge\}}^i + b_c\right) \quad (3)$$

Where W_c and b_c are the weight matrix and bias of the learnable FC layer, respectively. The concatenated feature representation $F_{\{merge\}}^i$ is fed into the FC layer and is then activated by the ReLU function. The ReLU function can be shown as in (4):

$$\mathrm{ReLU}(x) = \max(0, \ x) \quad (4)$$

is utilized to suppress unwanted values and maintain effective feature representations. The classification operation helps the model distinguish between changed and unchanged regions and finally improves the precision and recall of change detection.

3.2 Siamese Adaptive Fusion Network (SAFNet)

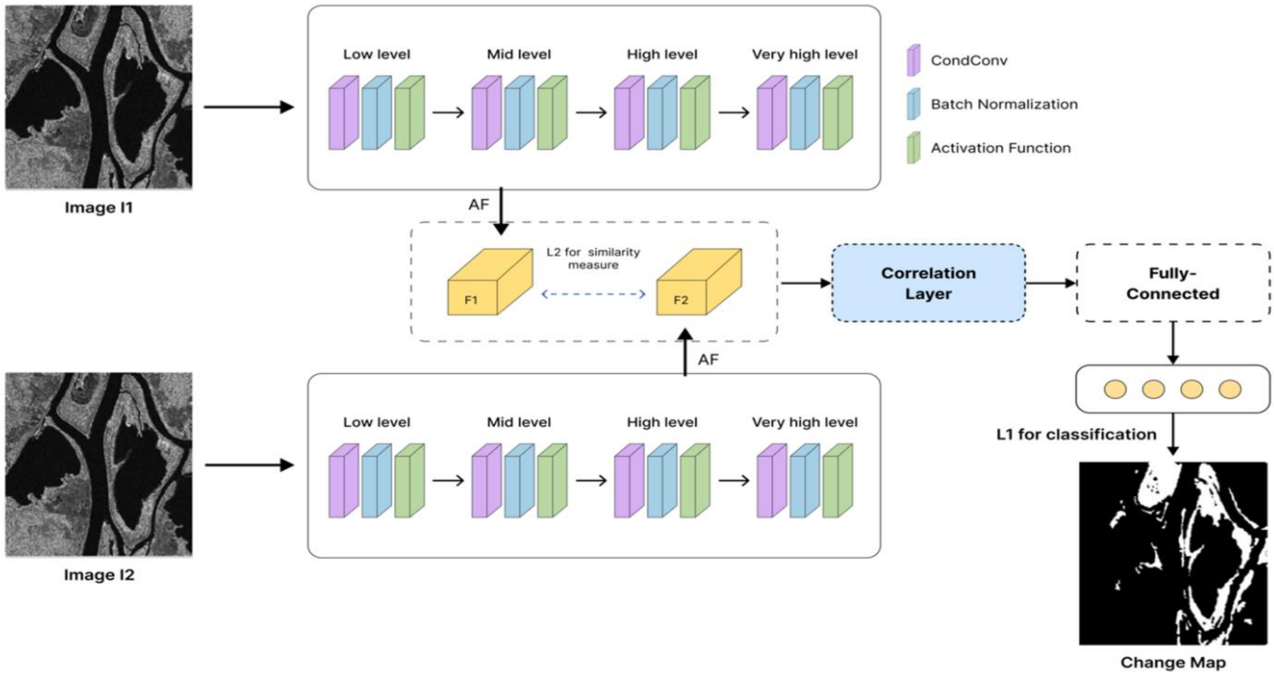

Figure 1 Siamese Adaptive Fusion Network (SAFNet) Framework

Figure 1 depicts a two-branch CNN-based scheme formulated for detecting change in SAR images. Such an approach helps efficient feature extraction, fusion, and classification in creating an authentic change map. Three principal phases include Feature Extraction, Feature Fusion, and Classification.

At the Feature Extraction and Representation Learning phase, the model is given a pair of SAR images acquired at two different time steps, referred to as Image I1 and Image I2. A deep convolutional neural network (CNN) with multiple levels of abstraction is used to process both images. All four of the network's hierarchical levels—Low-level, Mid-level, High-level, and Very High-level—learn different contextual and spatial characteristics. The low-level features learn edge, texture, and overall intensity variation, the mid-level features learn the structural and spatial relationships, and the high-level features learn the semantic information related to change detection. The very high-level features learn the discriminative feature representations to improve the discrimination between changed and unchanged areas. Conditional Convolutions (CondConv), Batch Normalization, and Activation Functions are called at each hierarchy for better learning efficiency as well as overfitting avoidance.

Once the features have been extracted, feature responses for both CNN branches, F1 and F2, are combined employing feature fusion via a measure-based similarity. This operation is employed to render the features discriminative enough to pick up on fine-grained differences between the two images. Similarity measurement uses an L2 distance function, which imposes a constraint to bring feature representations near to one another for regions that do not change and distant from one another for regions that change. This operation allows the network to focus on significant changes and eliminate redundant noise. The aggregated representation of the features is passed through a Correlation Layer, which boosts feature interaction and refines learned representations by picking up on pixel-wise relationships between the two feature maps.

After feature fusion, the Classification and Change Map Generation utilizes a Fully Connected (FC) Layer to label every pixel as "changed" or "unchanged." The FC layer uses a non-linear mapping of the fused

feature maps such that the model can precisely predict pixel-wise changes. Classification is optimized via an L1 loss function that reduces the absolute differences between ground truth labels and predicted labels. The model's ultimate output is a binary change map, with white pixels denoting changes that were detected and black pixels denoting regions that were unchanged.
This model employs deep feature representation in concert with correlation-based fusion to attain high-precision change detection in SAR images. Through the use of similarity measures and multi-scale feature extraction, the model is able to suppress noise, increase robustness, and enhance overall accuracy of change detection.

4. Experimental Results and Analysis

This part begins by introducing the experiment data and evaluation criteria. The elements that could impact SAFNet's performance will then be examined. Finally, a comparison with a number of cutting-edge techniques will be used to assess SAFNet's efficacy.
Two real-world SAR datasets were used in studies to evaluate SAFNet's performance for SAR image change detection.

4.1 Experiment Data and Evaluation Criteria

One of these is the Ottawa dataset as shown in Figure 2; it contains two images acquired using the Radarsat sensor in May and August of 1997. This dataset, as availed by the National Defense Research and Development Canada, indicates flooded regions. The spatial resolution of the Ottawa dataset is 10 meters while its dimensions are 290 × 350 pixels. The ground truth for this dataset was produced through a combination of prior knowledge and manual photo interpretation.
The second dataset is the S1GFloods dataset. The dataset is shown in Figure 3. The collection comprises ground truth maps for every pixel and worldwide pairs of high-resolution Sentinel-1 SAR pictures spanning 42 flood episodes from 2016 to 2022. Rivers, lakes, vegetation, urban and rural locations, and typical sources of flooding are all featured. This dataset offers vital information for creating plans to prevent and address flooding in the future.
To evaluate the performance, the two datasets are subjected to both qualitative and quantitative analysis. Visual comparison of the change maps produced by the suggested method with the corresponding ground truth photos is part of the qualitative study. False positives (FP), false negatives (FN), the Mean Intersection over Union (mIOU), the percentage of correct classification (PCC), and the Kappa coefficient (KC) are used in the quantitative evaluation. The number of unchanged pixels that are incorrectly altered is indicated by FP, whereas the number of changed pixels that are incorrectly categorized as unchanged is indicated by FN. OE is the total number of incorrectly classified pixels. i.e., FP + FN.

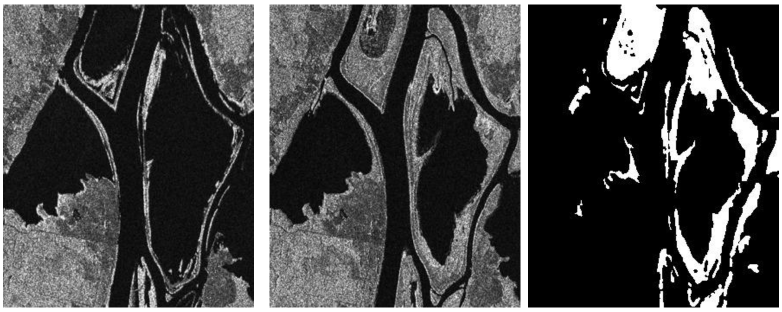

(a) (b) (c)

Figure 2 the Ottawa dataset. (a) Image acquired in May 1997. (b) Image acquired in August 1997. (c) Ground truth image.

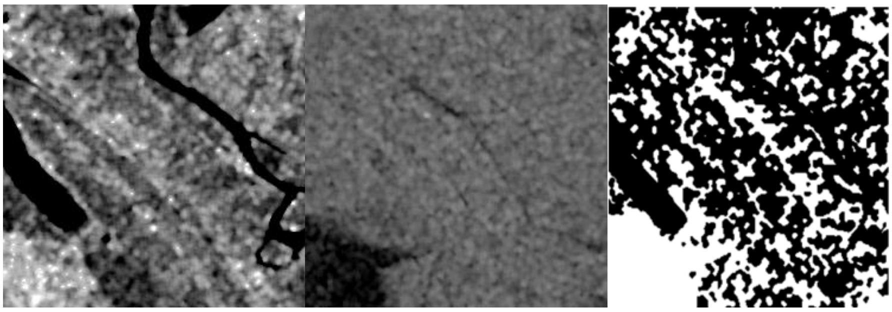

(a) (b) (c)

Figure 3 the S1GFlood dataset. (a) Image acquired in March 2017. (b) Image acquired in July 2017. (c) Ground truth image.

The PCC is calculated as in (5):

$$PCC = \frac{N_u + N_c - OE}{N_u + N_c} \times 100\% \qquad (5)$$

Where Nu denotes the total number of unchanged pixels in the ground truth image while Nc denotes the number of changed pixels. The mIOU is calculated as in (6):

$$mIOU = \frac{1}{C} \sum_{i=1}^{c} \frac{TPi}{TPi + FPi + FNi} \qquad (6)$$

Context of binary change detection, C represents the total number of classes, which is C=2. Class 1 corresponds to "changed" pixels and Class 2 corresponds to "unchanged" pixels.
The formula ensures the average Intersection over Union (IoU) is computed across all classes. For a single class, the IoU is as in (7):

$$IOU = \frac{Intersection}{Union} = \frac{TP}{TP + FP + FN} \qquad (7)$$

The KC is calculated as in (8):

$$KC = \frac{PCC - PRE}{1 - PRE} \times 100\% \qquad (8)$$

Where,

$$PRE = \frac{(Nc + FP - FN) \cdot Nc + (Nu + FN - FP) \cdot Nu}{(Nu + Nc) \cdot (Nu + Nc)} \qquad (9)$$

Here, we see that the value of KC is governed by FP and FN rather than by OE alone. Therefore, KC reflects the balance between FP and FN to some extent. More detailed, such knowledge should be used to yield acceptable KC values, and KC is more compelling evidence of the shift detection result than PCC or OE.

4.2 Experimental Results and Discussion

In order to validate the SAFNet, several Existing change detection methods are used for comparison. i.e., DCNet, DDNet, DDNet(WP), ESCNet, FCMMRF, FCMMRF(WP), Gabor PCANet, HFEMCRF, HFEMCRF(WP), NBRKLM, PCAKM, ResNet, RMGFDA, SAFNet. DCNet, a deep neural network, implements cascaded channel-weighting residual blocks for deeper feature extraction, and DDNet along with DDNet (WP), which implements two discriminators of which the last one includes post-processing for its results. In ESCNet, superpixel sampling networks are incorporated along with the Siamese U-Net to analyze relationships in multi-temporal images, and FCMMRF combines the fully convolutional networks with the Markov Random Fields for achieving spatial consistency with FCMMRF(WP), which includes the post-processing result for better precision. Gabor PCANet uses Gabor filters and PCANet for strong feature extraction, while HFEMCRF extracts hierarchical features using MRFs, with post-processing in HFEMCRF (WP). In NBRKLM, a neighborhood-based ratio operator is first applied for feature extraction and then k-means clustering for classification. PCAKM utilizes PCA for feature extraction and k-means clustering. ResNet makes use of ResNet-18 for pixel-wise classification, while RMGFDA uses random multi-graph frequency-domain analysis to classify changes with preservation of spatial relationships. Lastly, SAFNet adopts spatially adaptive fusion techniques for effective feature merging from multi-temporal images in order to improve the accuracy of SAR change detection.

4.2.1 Results on the Ottawa Dataset

Figure 4 summarizes the performance comparison of various methods on the Ottawa dataset. Table 1 lists the detailed evaluation criteria. PCAKM cannot identify which of the pixels did not change and paid a penalty of high FP rate. RMGFDA missed a large portion of changed pixels, resulting in higher FN. NBRKLM and Gabor PCANet balance FP and FN but still have missed changes in certain areas. HFEMCRF and its WP variant improve noise reduction and achieve competitive accuracy metrics. DDNet and FCMMRF(WP) show improvements in detecting changes but face challenges in balancing FP and FN. ESCNet performs best in capturing the changes, but it achieves the highest KC score at the cost of higher FP rates. The best-performing method is SAFNet, with the highest PCC and mIOU scores, which is able to accurately detect change regions with high precision and minimal noise. These results show the superiority of the novel design of SAFNet, especially its AF module and correlation analysis, in terms of superior change detection performance.

Table 1 Change Detection Results of Different Methods on the Ottawa Dataset

Methods	FP	FN	KC (%)	mIOU (%)	PCC (%)
DCNet	22	2546	93.60	80.41	98.60
DDNET	**2**	6813	90.68	80.52	95.45
DDNET(WP)	1237	1430	80.95	85.60	95.90
ESCNet	5325	1573	**99.86**	83.38	96.95
FCMMRF	13	3914	91.70	80.97	98.24
FCMMRF(WP)	3038	1128	87.50	86.25	96.69

Gabor PCANET	1080	1230	83.28	89.64	95.63
HFEMCRF	418	478	85.67	**93.94**	98.63
HFEMCRF(WP)	996	826	90.42	90.35	97.22
NBRKLM	296	1758	96.23	85.98	96.87
PCAKM	420	4878	91.30	83.96	95.91
RESNET	918	4636	95.45	80.35	96.52
RMGFDA	21	1685	99.68	82.72	96.81
SAFNet	1279	**62**	91.09	91.65	**99.35**

4.2.2 Results on the S1GFloods Dataset:

Figure 5 summarizes the performance comparison of various methods on the S1GFloods dataset. Table 2 lists the detailed evaluation criteria. PCAKM exhibits a high FP rate, which indicates an inability to effectively distinguish unchanged pixels. RMGFDA misses a significant number of changed pixels, resulting in a high FN rate. NBRKLM and Gabor PCANet strike a balance between FP and FN miss certain changes. HFEMCRF and its WP variant achieve notable noise reduction and competitive accuracy. DDNet improves the detection of changes but struggles with balancing FP and FN. FCMMRF (WP) achieves the highest KC score by accurately capturing change areas but suffers from a relatively higher FN rate. ESCNet performs well overall but has a higher FP rate, which impacts precision. The best-performing method is SAFNet, with the highest PCC and mIOU scores. It demonstrates exceptional performance in detecting change regions with high accuracy and minimal noise. These results highlight the strength of SAFNet's advanced feature extraction and correlation analysis capabilities, which deliver state-of-the-art performance for change detection in SAR images.

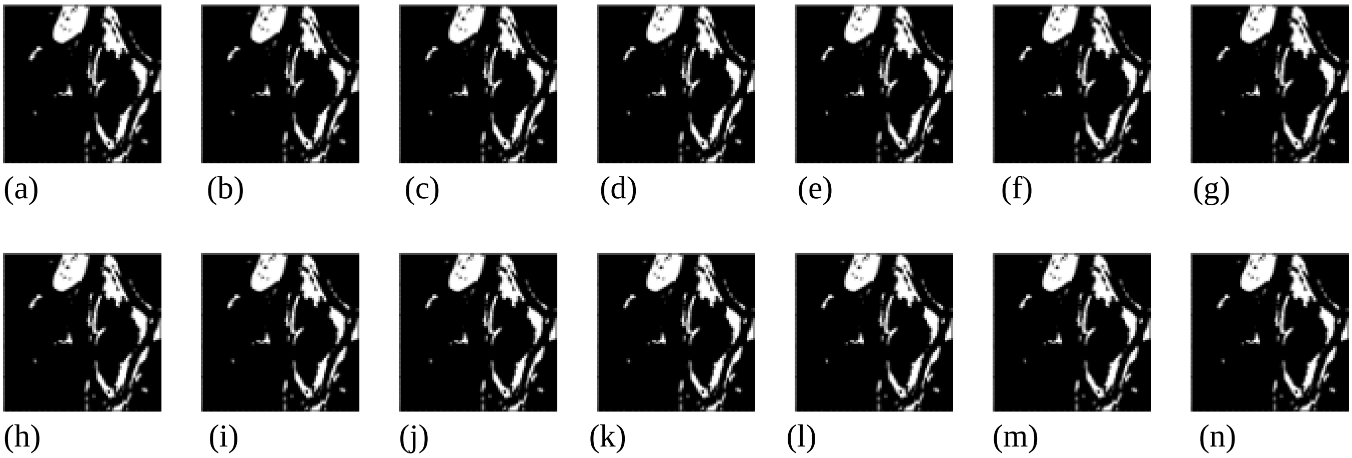

Figure 4 Visualized results of change detection methods on the Ottawa dataset. (a) DCNet (b) DDNet (c) DDNet(WP) (d) ESCNet (e) FCMMRF (f) FCMMRF(WP) (g) GaborPCANet (h) HFEMCRF (i) HFEMCRF(WP) (j) NBRELM (k) PCAKM (l) RESNET (m) RMGFDA (n) SAFNET

Table 2 Change Detection Results of Different Methods on the S1GFloods Dataset

Methods	FP	FN	KC (%)	mIOU (%)	PCC (%)
DCNet	14370	2640	73.60	56.84	78.38
DDNET	17560	2698	80.68	60.19	77.68
DDNET(WP)	8560	18520	70.95	50.95	69.30
ESCNet	16839	3860	79.86	59.36	71.32
FCMMRF	**206**	15480	71.70	57.13	63.33
FCMMRF(WP)	5092	12860	**87.50**	56.18	68.62
Gabor PCANET	17999	3654	63.28	51.53	75.28
HFEMCRF	6024	12540	65.67	59.17	64.32
HFEMCRF(WP)	19604	6452	80.42	60.17	76.56
NBRKLM	15638	1284	60.23	57.99	78.39
PCAKM	18906	1984	61.30	55.94	76.85
RESNET	5862	15631	65.45	60.13	68.09
RMGFDA	14890	2380	69.68	53.51	78.06
SAFNet	12952	**1080**	71.09	**65.80**	**80.24**

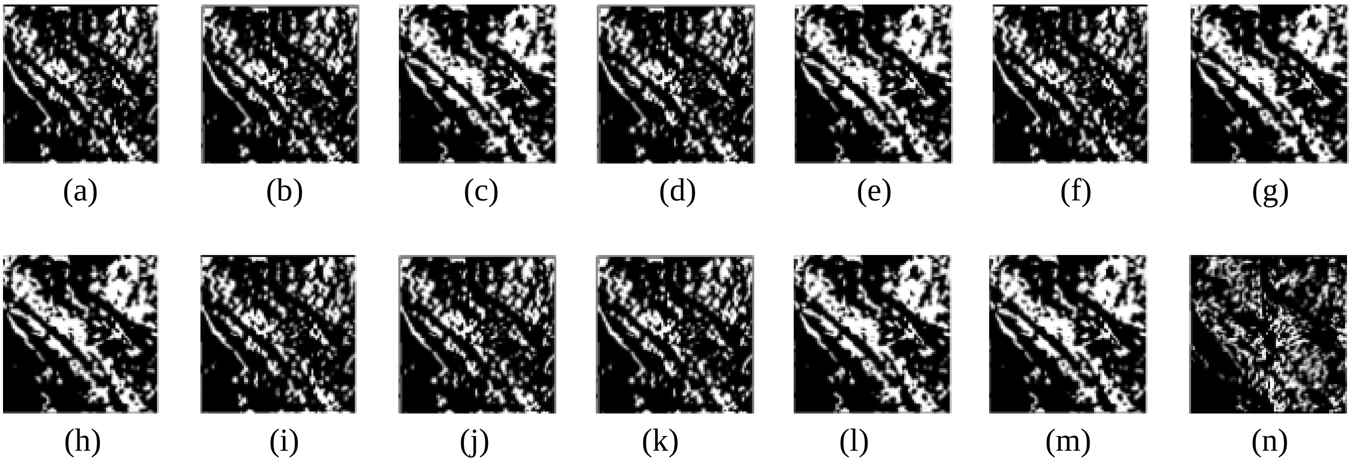

Figure 5 Visualized results of change detection methods on the S1GFloods dataset. (a) DCNet (b) DDNet (c) DDNet(WP) (d) ESCNet (e) FCMMRF (f) FCMMRF(WP) (g) GaborPCANet (h) HFEMCRF (i) HFEMCRF(WP) (j) NBRELM (k) PCAKM (l) RESNET (m) RMGFDA (n) SAFNET

Figure 6(a) displays the comparison of KC values of different change detection techniques. The outcome indicates that the proposed technique obtains better consistency and robustness, having higher KC values on both datasets than the conventional methods. Figure 6(b) displays the PCC values of various methods, which shows that the proposed model always outperforms other methods. The greater the PCC values, the better the accuracy of change detection, verifying the effectiveness of the model under different circumstances.

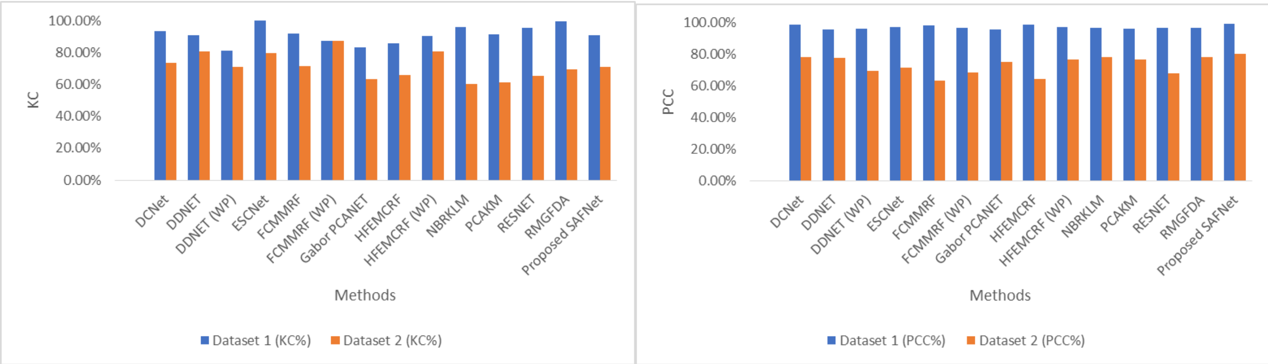

(a) (b)

Figure 6 Comparative performance evaluation of different change detection methods on two datasets. (a) Kappa Coefficient (KC) comparison. (b) Percentage of Correct Classification (PCC) comparison.

5. Conclusions

Deep learning techniques for SAR image change detection have advanced significantly. It is still difficult to achieve greater discriminative feature representation. The correlation layer integrates features from two-branch networks, guided by a similarity measure, improving the separation of changed and unchanged pixels. This paper introduces the AF module, which can adaptively fuse multi-level features, enhancing meaningful ones and suppressing irrelevant ones. The network is further optimized for reliable feature extraction using classification loss. SAFNet is beneficial for a variety of circumstances since it outperforms state-of-the-art techniques in terms of quantitative measurements and visual outputs. Large-scale, long-term applications will advance further due to developments in multisource image change detection and high-resolution Earth observation.

References:

1. Y. Gao, F. Gao, J. Dong, Q. Du, and H.-C. Li, "Synthetic Aperture Radar Image Change Detection via Siamese Adaptive Fusion Network," IEEE J. Sel. Top. Appl. Earth Obs. Remote Sens., vol. 14, pp. 10748–10760, 2021.
2. L. Li, H. Ma, X. Zhang, X. Zhao, M. Lv, and Z. Jia, "Synthetic Aperture Radar Image Change Detection Based on Principal Component Analysis and Two-Level Clustering," Remote Sens., vol. 16, no. 11, p. 1861.
3. X. Qu, F. Gao, J. Dong, Q. Du, and H.-C. Li, "Change Detection in Synthetic Aperture Radar Images Using a Dual-Domain Network," IEEE Geosci. Remote Sens. Lett., vol. 19, pp. 1–5, 2022.
4. D. Meng, F. Gao, J. Dong, Q. Du, and H.-C. Li, "Synthetic Aperture Radar Image Change Detection via Layer Attention-Based Noise-Tolerant Network," IEEE Geosci. Remote Sens. Lett., vol. 19, pp. 1–5, 2022.
5. Y. Gao, F. Gao, J. Dong, and S. Wang, "Change Detection From Synthetic Aperture Radar Images Based on Channel Weighting-Based Deep Cascade Network," IEEE J. Sel. Top. Appl. Earth Obs. Remote Sens., vol. 12, no. 11, pp. 4517–4529, Nov. 2019.
6. J. Wang, F. Gao, J. Dong, Q. Du, and H.-C. Li, "Change Detection From Synthetic Aperture Radar Images via Dual Path Denoising Network," IEEE J. Sel. Top. Appl. Earth Obs. Remote Sens., vol. 15, pp. 2667–2680, 2022.

7. H. Dong, W. Ma, Y. Wu, M. Gong, and L. Jiao, “Local Descriptor Learning for Change Detection in Synthetic Aperture Radar Images via Convolutional Neural Networks,” IEEE Access, vol. 7, pp. 15389–15403, 2019.
8. J. Wang, F. Gao, J. Dong, S. Zhang, and Q. Du, “Change Detection From Synthetic Aperture Radar Images via Graph-Based Knowledge Supplement Network,” IEEE J. Sel. Top. Appl. Earth Obs. Remote Sens., vol. 15, pp. 1823–1836, 2022.
9. H. Dong, W. Ma, L. Jiao, F. Liu, and L. Li, “A Multiscale Self-Attention Deep Clustering for Change Detection in SAR Images,” IEEE Trans. Geosci. Remote Sens., vol. 60, pp. 1–16, 2022.
10. Q. Wang et al., “High-Resolution Remote Sensing Image Change Detection Method Based on Improved Siamese U-Net,” Remote Sens., vol. 15, no. 14, p. 3517, Jul. 2023.
11. B. Cui, Y. Zhang, L. Yan, J. Wei, and H. Wu, “An Unsupervised SAR Change Detection Method Based on Stochastic Subspace Ensemble Learning,” Remote Sens., vol. 11, no. 11, p. 1314, Jun. 2019.
12. S. T. Seydi, R. Shah-Hosseini, and M. Amani, “A Multi-Dimensional Deep Siamese Network for Land Cover Change Detection in Bi-Temporal Hyperspectral Imagery,” Sustainability, vol. 14, no. 19, p. 12597, Oct. 2022.
13. S. Hafner, Y. Ban, and A. Nascetti, “Semi-Supervised Urban Change Detection Using Multi-Modal Sentinel-1 SAR and Sentinel-2 MSI Data,” Remote Sens., vol. 15, no. 21, p. 5135, Oct. 2023.
14. Z. Liang, B. Zhu, and Y. Zhu, “High resolution representation-based Siamese network for remote sensing image change detection,” IET Image Process., vol. 16, no. 9, pp. 2506–2517, Jul. 2022.
15. H. Zhang, Z. Lin, F. Gao, J. Dong, Q. Du, and H.-C. Li, “Convolution and Attention Mixer for Synthetic Aperture Radar Image Change Detection,” IEEE Geosci. Remote Sens. Lett., vol. 20, pp. 1–5, 2023.
16. J. Wang, X. Wang, L. Guo, Y. Xu, Z. Lu, and B. Chen, “Clustering-segmentation network: a parallel dual-branch synthetic aperture radar image change detection framework,” Int. J. Remote Sens., vol. 44, no. 5, pp. 1579–1610, Mar. 2023.
17. V. N. S. Vudattu and U. C. Pati, “Change Detection in Synthetic Aperture Radar Images based on a Spatial Pyramid Pooling Attention Network (SPPANet),” Remote Sens. Lett., vol. 14, no. 11, pp. 1139–1149, Nov. 2023.
18. H. Dong et al., “Dynamic Bilinear Fusion Network for Synthetic Aperture Radar Image Change Detection,” IEEE Geosci. Remote Sens. Lett., vol. 22, pp. 1–5, 2025.
19. H. Zhang, Z. Lin, F. Gao, J. Dong, Q. Du, and H.-C. Li, “Convolution and Attention Mixer for Synthetic Aperture Radar Image Change Detection,” IEEE Geosci. Remote Sens. Lett., vol. 20, pp. 1–5, 2023.
20. C. Tao et al., “A Siamese Network with a Multiscale Window-Based Transformer via an Adaptive Fusion Strategy for High Resolution Remote Sensing Image Change Detection,” Remote Sens., vol. 15, no. 9, p. 2433, May 2023.
21. Z. Yang, Y. Wu, M. Li, X. Hu, and Z. Li, “Unsupervised Difference-Guided Adaptive Fusion Network for Change Detection in PolSAR Images,” IEEE Trans. Geosci. Remote Sens., vol. 62, pp. 1–16, 2024.
22. J. Wang, X. Wang, L. Guo, Y. Xu, Z. Lu, and B. Chen, “Clustering-segmentation network: a parallel dual-branch synthetic aperture radar image change detection framework,” Int. J. Remote Sens., vol. 44, no. 5, pp. 1579–1610, Mar. 2023.

23. X. Long, W. Zhuang, M. Xia, K. Hu, and H. Lin, “SASiamNet: Self-Adaptive Siamese Network for Change Detection of Remote Sensing Image,” IEEE J. Sel. Top. Appl. Earth Obs. Remote Sens., vol. 17, pp. 1021–1034, 2024.
24. H. Li, B. Zou, L. Zhang, and J. Qin, “Semi-Supervised SAR Image Change Detection via Structure-Optimized Complex-Valued Graph Contrastive Learning,” IEEE Geosci. Remote Sens. Lett., vol. 21, pp. 1–5, 2024.
25. J. Wang, F. Gao, J. Dong, S. Zhang, and Q. Du, “Change Detection From Synthetic Aperture Radar Images via Graph-Based Knowledge Supplement Network,” IEEE J. Sel. Top. Appl. Earth Obs. Remote Sens., vol. 15, pp. 1823–1836, 2022.
26. V. N. S. Vudattu and U. C. Pati, “Change Detection in Synthetic Aperture Radar Images based on a Spatial Pyramid Pooling Attention Network (SPPANet),” Remote Sens. Lett., vol. 14, no. 11, pp. 1139–1149, Nov. 2023.
27. C. Wang, W. Su, and H. Gu, “A joint change detection method on complex-valued polarimetric synthetic aperture radar images based on feature fusion and similarity learning,” Int. J.Remote Sens., vol. 42, no. 13, pp. 4864–4881, Jul. 2021.
28. B. Pandeeswari, J. Sutha, and M. Parvathy, “A novel synthetic aperture radar image change detection system using radial basis function-based deep convolutional neural network,” J. Ambient Intell. Humaniz. Comput., vol. 12, no. 1, pp. 897–910, Jan. 2021.
29. J. Chen et al., “DPFF-Net: Dual-Polarization Image Feature Fusion Network for SAR Ship Detection,” IEEE Trans. Geosci. Remote Sens., vol. 61, pp. 1–14, 2023.
30. P. Chen et al., “ADF-Net: An Attention-Guided Dual-Branch Fusion Network for Building Change Detection near the Shanghai Metro Line Using Sequences of Terra SAR-X Images,” Remote Sens., vol. 16, no. 6, p. 1070, Mar. 2024.
31. T. Zhan, Q. Dang, and Y. Zhu, “Neighborhood Difference-Based Self-Supervised Network for Detecting Small Changes From Synthetic Aperture Radar Images,” IEEE Geosci. Remote Sens. Lett., vol. 21, pp. 1–5, 2024.
32. C. Chen, Y. Zheng, X. Jiang, and X. Liu, “SAR Image Change Detection Via UR-ISTA,” in IGARSS 2022 - 2022 IEEE International Geoscience and Remote Sensing Symposium, Kuala Lumpur, Malaysia: IEEE, Jul. 2022, pp. 679–682.